

K-shell photoabsorption of the N₂ molecule

C. T. Chen, Y. Ma, and F. Sette

AT&T Bell Laboratories, Murray Hill, New Jersey 07974

(Received 8 May 1989)

The K-shell photoabsorption spectrum of the N₂ molecule, recorded with unprecedented energy resolution and statistical accuracy, reveals several new Rydberg transitions and double-excitation states. The nearly identical term values, vibrational frequencies, and internuclear separations of the 1s-excited states of N₂ and of the 2π-excited states of NO, allow for a complete peak assignment for the N₂ Rydberg series and strongly support both the core-hole localization picture and equivalent-core model. Subtle differences are related to the final-state charge distribution in the vicinity of the nuclei and to the bonding character of the valence orbitals.

The inner-shell absorption process is a unique probe to investigate the internuclear potential, the core-hole decay mechanisms, and the electronic configuration of highly excited molecules. Many physical concepts, such as the Born-Oppenheimer approximation, the Frank-Condon principle, and the equivalent-core model, are severely challenged when applied to this core process. The K-shell absorption spectrum of the N₂ molecule, with its many spectral features, has been widely used as a prototype system to test these ideas. In spite of advances in photoabsorption and electron energy-loss spectroscopies, the K-shell excitation spectrum of this molecule¹⁻¹⁰ is still veiled as a consequence of insufficient energy resolution or signal-to-noise ratio.

To reveal the absorption structure in better detail and to examine the equivalent-core model with improved accuracy, we have measured the K-shell photoabsorption spectra of the N₂ molecule using high-resolution soft-x-ray synchrotron radiation. With much improved photon energy resolution and data statistics, many new excitation lines are observed, and high-precision spectroscopic constants, including term value, vibrational frequency, and internuclear separation, are deduced. By comparing with the optical-transition data of NO, we have unambiguously determined the final-state configurations of the 1s-excited Rydberg states of N₂ and resolved uncertainties persisting in the literature. The core-hole localization picture and equivalent-core model are found to be valid to a high degree. A subtle deviation from this model is also observed, and is explained by considering the charge differences in the vicinity of the nuclei. The effect on the internuclear potential of exciting an electron in the 1π_g^{*} (equivalent to the 2π in NO) or in a Rydberg orbital is investigated by comparing the spectroscopic constants of different excited states of N₂.

This experiment was performed using the newly constructed Bell Laboratories' high-resolution Dragon soft-x-ray beam line located at the National Synchrotron Light Source, Brookhaven National Laboratory.¹¹ In these measurements, the energy resolution was set to about 40 meV. The spectra were taken with the transmission method recording the electrons generated by the transmitted photons impacting on a gold target. They were also taken at different gas pressures to control the saturation effect. For our 10-cm-long gas cell, the opti-

mized gas pressure was about 0.1 torr for the N 1s → 1π_g^{*} absorption region and about 1 torr for the other energy regions.

Figure 1 shows the wide-range K-shell photoabsorption spectrum of the N₂ molecule. This spectrum is the result of combining measurements taken at two different gas pressures. The peaks between 400 and 402 eV are the N 1s → 1π_g^{*} excitation and its vibrational sideband. The features observed between 406 and 410 eV are the N 1s → Rydberg series transitions. The N 1s ionization threshold occurs at 409.938 eV.¹² The area between 413 and 416 eV has been assigned in the literature to double-excitation states that are the shakeups associated with the N 1s → 1π_g^{*} transition. The broad peak at 420 eV is the σ-shape resonance. The absolute photon energy scale is calibrated using the value of 401.10 eV for the second peak in the N 1s → 1π_g^{*} excitation, which was previously determined by high-resolution electron-energy-loss spectroscopy¹⁰ (EELS).

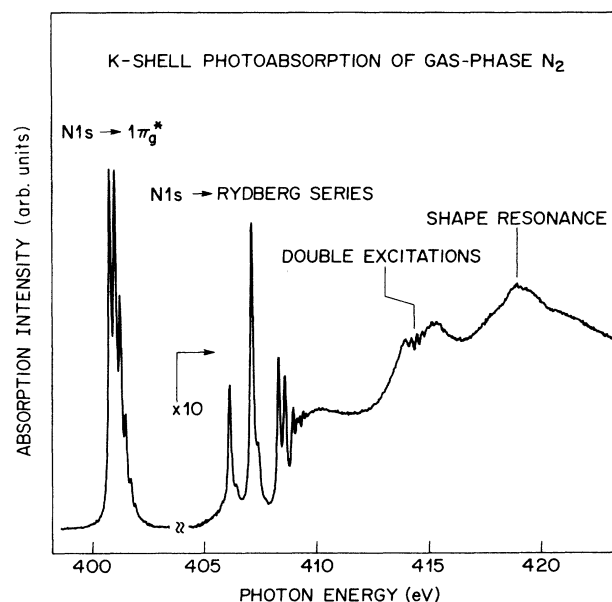


FIG. 1. K-shell photoabsorption spectrum of gas-phase N₂.

The eight vibrational levels observed in the $N\ 1s \rightarrow 1\pi_g^*$ absorption spectrum, shown in Fig. 2(a), confirm the multiple-peak structure previously recorded by EELS measurements.^{6,9,10} The electronic transition energy of the $0 \rightarrow 0$ vibrational level ν_{00} , the vibrational constants ω_e and $\omega_e x_e$, the full width at half maximum (FWHM) lifetime width Γ , and the relative intensities of these levels are deduced from the data by least-squares curve fitting using Voigt functions and a linear background. The deduced values for ν_{00} , ω_e , $\omega_e x_e$, and Γ are 400.868 eV, 235.2 ± 0.5 , 1.9 ± 0.5 , and 132 ± 8 meV, respectively. The intensities relative to the first peak are 1.000, 0.968, 0.564, 0.250, 0.088, 0.030, 0.011, and 0.004. Using the Frank-Condon principle and a Morse potential, we obtain an internuclear separation r_e of 1.164 ± 0.001 Å. These spectroscopic constants are consistent with the published values but the improved data quality gives them higher precision.^{6,9}

Figure 2(b) shows the absorption spectrum of the $N\ 1s \rightarrow$ Rydberg transitions. Twelve peaks are readily observed in this spectrum. To deduce the spectroscopic constant from the data, a least-squares curve fitting was performed. In addition to the functions mentioned above, an integral of the Voigt function was included to represent the ionization threshold, and the maximum of its first derivative was fixed at 409.938 eV. Initially, we used only twelve peaks and the result was very satisfactory except for a few tenths of eV near 407.3 and 408.9 eV, and the ionization threshold. The high quality of our data and the confidence we have on using the Voigt function as the peak profile, justified to refit the data by adding two peaks, one near 407.3 and the other near 408.9 eV. Two peaks were also added near the ionization threshold to represent those unresolvable Rydberg states which are converging toward the continuum. The excellent quality of the fit is evident by the close match between the dots and the solid curve shown in Fig. 2(b). The energy positions and the relative intensities obtained from this fit are listed in columns 2 and 3 of Table I.¹³

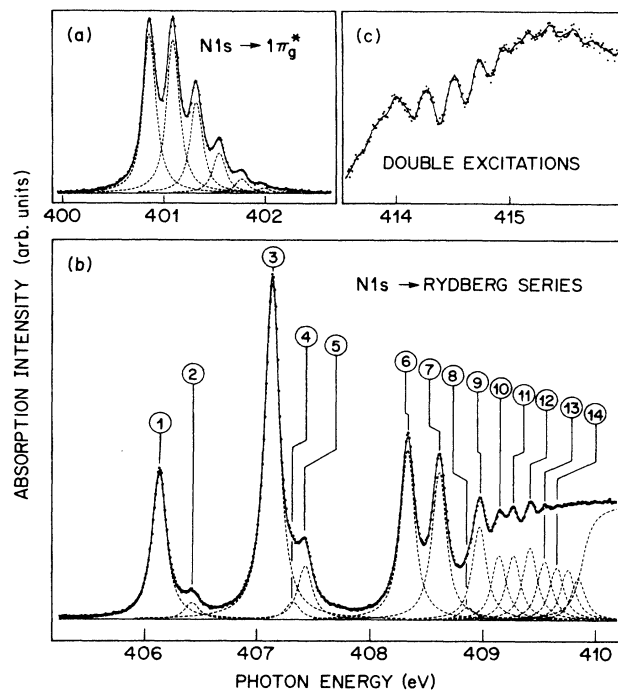


FIG. 2. Photoabsorption spectra of (a) $N\ 1s \rightarrow 1\pi_g^*$, (b) $N\ 1s \rightarrow$ Rydberg series, and (c) double-excitation transitions of gas-phase N_2 . Dots represent the experimental data. The solid curves in (a) and (b) are the result of the fitting procedure explained in the text and the dashed curves are the individual Voigt profile determined from the fit. The solid curve in (c) is a smoothing of the data.

According to the equivalent-core model, the final-state electronic configuration of a $N\ 1s \rightarrow$ Rydberg excitation in N_2 is identical to that of its corresponding $2\pi \rightarrow$ Rydberg excitation in NO, except for the differences in nuclear mass and charge distribution in the vicinity of the nuclei. The optical transition data of NO can then be uti-

TABLE I. The transition energy, relative intensity, and the term values of the $N\ 1s \rightarrow$ Rydberg transitions of N_2 . The term values and final-state configurations of the corresponding $2\pi \rightarrow$ Rydberg transitions of NO are also listed for comparison. All energies are listed in eV.

n	N_2 ($N\ 1s\ BE = 409.938$)			NO ($2\pi\ BE = 9.264$)	
	E_n	I_n/I_1	Term	Term	Final state
1	406.150	1.000	3.788	3.799	$A^2\Sigma^+$ ($3s\sigma$)
2	406.439	0.115	3.499		$A^2\Sigma^+$ $0 \rightarrow 1$
3	407.115	2.307	2.793	2.786	$C^2\Pi_r$ ($3p\pi$)
4	407.329	0.120	2.609	2.672	$D^2\Sigma^+$ ($3p\sigma$)
5	407.441	0.369	2.497		$C^2\Pi_r$ $0 \rightarrow 1$
6	408.347	1.164	1.591	1.587	$F^2\Sigma^+$ ($4s\sigma$)
7	408.628	1.012	1.310	1.309	$K^2\Pi$ ($4p\pi$)
8	408.877	0.087	1.061		$K^2\Pi$ $0 \rightarrow 1$
9	408.987	0.638	0.951	0.955	$S^2\Sigma^+$ ($5s\sigma$)
10	409.161	0.443	0.777	0.768	$Q^2\Pi$ ($5p\pi$)
11	409.288	0.442	0.650	0.605	$T^2\Sigma^+$ ($6s\sigma$)
12	409.436	0.496	0.502	0.508	$W^2\Pi$ ($6p\pi$)
13	409.565	0.401	0.373	0.419	$Z^2\Sigma^+$ ($7s\sigma$)
14	409.674	0.360	0.264		

lized to identify the peaks shown in Fig. 2(b) and to investigate the validity of this model. To compare these equivalent-core states, the term values of the N $1s \rightarrow$ Rydberg excited states of N₂ and those of the $2\pi \rightarrow$ Rydberg excited states of NO are listed respectively in column 4 and 5 of Table I. The term values of N₂ were calculated as the difference between the E_n values listed in column 1 and the N $1s$ binding energy (BE) of 409.938 eV, while those of NO by subtracting the ν_{00} listed in Ref. 14 from the 2π BE of 9.2644 eV. Inspecting the term values listed in columns 4 and 5, we found a striking match, precise to within 10 meV, between most of the equivalent-core states of N₂ and NO. The less precise match, within 40–60 meV, for peaks 4, 11, and 13 can be accounted for by the facts that it is more difficult to deduce the energy position for weak peaks, and that there is a large energy uncertainty in the reported value for the $T^2\Sigma^+$ state of NO.¹⁴ By subtracting the transition energy of the vibrational ground state of the N $1s \rightarrow 1\pi_g^*$ excitation, denoted as NN*, from the N $1s$ ionization threshold of N₂, the term value (or the first ionization potential) of NN* is calculated to be 9.070 eV, which is 0.194 eV smaller than that of the ground state of NO. This 0.194-eV energy deficit will be addressed later. The overall agreement, however, strongly supports the core-hole localization picture and the equivalent-core model, and indicates that electronic configuration of the N $1s \rightarrow$ Rydberg excited states are identical to the corresponding ones listed in the last column of Table I for NO, except for the spin multiplicity being singlet instead of doublet. Since we favor the core-hole localization picture, the parity quantum number is omitted.

The presence of the weak peak 4, necessary to explain the data in its corresponding energy region, resolves the long-standing assignment uncertainties persisting in the literature for the 407.3-eV shoulder (as seen in lower quality spectra). A controversy centered on whether to interpret this feature as the N $1s^{-1}(3p\sigma)$ state or as the $0 \rightarrow 1$ vibrational excitation of N $1s^{-1}(3p\pi)$ state.^{2,5,8} Our data show that both excitations are present with the N $1s^{-1}(3p\sigma)$ being peak 4 and the vibrational excitation of the N $1s^{-1}(3p\pi)$ being peak 5. By noticing the large intensities observed in the N $1s \rightarrow 3s\sigma$ and N $1s \rightarrow 5s\sigma$ transitions, peaks 1 and 9, and the term values from NO

optical transition measurements, E and F states of Ref. 14, it is very tempting to assign peak 6 to be predominantly the N $1s \rightarrow 4s\sigma$ transition instead of the N $1s \rightarrow 3d\pi$ (Refs. 8 and 15) or N $1s \rightarrow 3d\delta$ (dipole forbidden) transition. This peak assignment then suggests also that the final-state configurations for the E and F states observed in the optical transition of NO should be exchanged as $E^2\Delta(3d\delta)$ and $F^2\Sigma^+(4s\sigma)$.¹⁴

Two $0 \rightarrow 1$ vibrational levels, peaks 2 and 4, are observed next to their corresponding $0 \rightarrow 0$ transition, peaks 1 and 3. The ω_e , r_e , and Γ for the various N $1s$ -excited states of N₂ and for the equivalent-core states of NO are listed in Table II. They are deduced using the same procedure mentioned before. The close match in the values of ω_e and r_e between the equivalent-core state of N₂ and NO, constitutes an independent evidence for the validity of both the core-hole localization picture and the equivalent-core model. The small differences between equivalent-core states in the two molecules and between different states in the same molecule can be related, respectively, to the charge differences in the vicinity of the nuclei, and to the bond character difference between the $1\pi_g^*$ and Rydberg orbitals. When going from $1\pi_g^*$ to Rydberg states, the bond strength within the molecule increases, i.e., ω_e is larger and r_e is smaller, because the $1\pi_g^*$ orbital has a strong antibonding character, while the Rydberg electron, being more delocalized, has either a non-bonding or slight bonding character. This is also evident in NO by comparing the ω_e and r_e of the ground state with the 2π -excited Rydberg states. Similarly, the increase in ω_e and decrease in r_e observed going from the $3s\sigma$ to the $3p\pi$ state of both NN* and NO, implies that the internuclear potential is further strengthened as a consequence of the slight bonding character of the $3p\pi$ orbital.

The systematic ~ 9 -meV increase of ω_e and ~ 0.013 -Å decrease of r_e between equivalent-core states in going from N₂ to NO can be rationalized by considering the charge differences in the vicinity of nuclei. Qualitatively speaking, the net effect of an extra proton in the nucleus and an electron in its $1s$ orbital, such as in the case of NO compared to NN*, is an attractive potential experienced by the valence electrons. This effect, determined by the penetration of the valence orbitals through the $1s$ wave

TABLE II. ω_e , r_e , and Γ for four N $1s$ -excited states of N₂ and for their equivalent-core states of NO. The ω_e for NO have been corrected for the reduced mass of N₂ by multiplying $(\frac{16}{15})^{1/2}$ to their original values. The value in parentheses are obtained by interpolation from the corresponding NO values. When calculating the ω_e for the N₂ Rydberg states, the $\omega_e x_e$ was assumed to be the same as that of the corresponding optical transition in NO. The accuracy including this approximation is ± 2 meV. The accuracy for relative values of Γ is ± 3 meV, while the absolute accuracy is ± 8 meV including the uncertainty in the instrumental bandwidth. The r_e of core-excited N₂ are precise to within ± 0.001 Å.

N ₂ state	ω_e (meV)		r_e (Å)		Γ (meV)
	N ₂	NO	N ₂	NO	N ₂
N $1s^{-1}(1\pi_g^*)$	235.2	243.8	1.1641	1.1508	132
N $1s^{-1}(3s\sigma)$	293.0	304.1	1.0767	1.0634	136
N $1s^{-1}(3p\pi)$	299.9	306.6	1.0734	1.062	136
N $1s^{-1}$	(293.2)	304.3	(1.0765)	1.0632	...

function, is due to the fact that a $1s$ electron cannot fully screen the extra positive charge in the nucleus. The bonding within the molecule is therefore increased in NO with respect to N_2 , and this is responsible for the observed larger ω_e and a smaller r_e . This effect and the fact that the N $1s$ wave function overlaps appreciably with the 2π wave function but negligibly with the diffused Rydberg orbitals, is also responsible for the first ionization potential of NN^* being 0.194 eV smaller than that of the ground state of NO.

The double-excitation region of the N_2 spectrum is shown in Fig. 2(c). Here we observe a previously unrecognized multiple-peak structure. This structure is composed of nine peaks, observed at photon energy 13.14, 13.40, 13.65, 13.87, 14.08, 14.30, 14.49, 14.70, and 14.85 eV with respect to the ν_{00} value of NN^* . These values are in the energy region of the 1π and 5σ Rydberg transitions of NO,^{14,16} and therefore this multiple-peak structure is identified as the 1π ($1\pi_u^*$ in NN^*) and 5σ ($3\sigma_g^*$ in NN^*) to Rydberg shakeup states associated with the N $1s \rightarrow 1\pi_g^*$ transition of N_2 . It is difficult to give an assignment for each peak by comparing to the NO data, because the shake-up process in N_2 is a monopole transition while the optical excitation in NO is a dipole transition. Nevertheless, based on the Frank-Condon principle and the notion that a shakeup transition could weaken the bond strength and consequently increase the internuclear separation of NN^* , these shakeup states should have a vibrational sideband comparable to or even stronger than that

of the N $1s \rightarrow 1\pi_g^*$ transition. It is very plausible then that the majority of these peaks are the vibrational sidebands of the shakeup states. Noting that the energy separations between the first five peaks is larger than that of the rest of peaks, it is very tempting to assign the first five peaks as the $5\sigma \rightarrow 3s\sigma$ and the rest of them as the $1\pi \rightarrow 3p\pi$ shakeup states. This is because the 5σ orbital, contrary to the 1π orbital, has a nonbonding character, and consequently the bond strength in the molecule is weakened more in the $1\pi \rightarrow 3p\pi$ shakeup state.

In conclusion, high-resolution soft-x-ray synchrotron radiation has been utilized to reveal many new states in the K -shell excitations of the N_2 molecule. A complete peak assignment, that resolves previous uncertainties, is given for the Rydberg series. The core-hole localization picture as well as the equivalent-core model are demonstrated to be valid to a high degree. Subtle differences in ω_e and r_e among N $1s$ excited states of N_2 and between the equivalent-core states of N_2 and of NO are clearly observed, and are explained in terms of the properties of the valence orbitals' bonding character and of the charge differences in the vicinity of the nuclei.

We acknowledge N. V. Smith for a critical reading of the manuscript, and E. Chaban and G. Meigs for valuable technical assistance. This work was done at the National Synchrotron Light Source, which is supported by the U.S. Department of Energy under Contract No. DE-AC02-76CH00016.

¹J. Prins, *Physica* **1**, 1174 (1934).

²M. Nakamura, M. Sasanuma, S. Sato, M. Watanabe, H. Yamashita, Y. Iguchi, A. Ejiri, S. Nakai, S. Yamaguchi, T. Sagawa, Y. Nakai, and T. Oshio, *Phys. Rev.* **178**, 80 (1969).

³M. J. Van der Wiel, T. M. El-Sherbini, and C. E. Brion, *Chem. Phys. Lett.* **7**, 161 (1970).

⁴G. R. Wight, C. E. Brion, and M. J. Van der Wiel, *J. Electron. Spectrosc.* **1**, 457 (1972).

⁵A. S. Vinogradov, B. Shlarbaum, and T. M. Zimkina, *Opt. Spectrosc.* **36**, 383 (1974).

⁶G. C. King, F. H. Read, and M. Tronc, *Chem. Phys. Lett.* **52**, 50 (1977).

⁷A. Bianconi, H. Petersen, F. C. Brown, and R. Z. Bachrach, *Phys. Rev. A* **17**, 1907 (1978).

⁸M. Tronc, G. C. King, and F. H. Read, *J. Phys. B* **13**, 999 (1980).

⁹A. P. Hitchcock and C. E. Brion, *J. Electron. Spectrosc.* **18**, 1 (1980).

¹⁰R. N. S. Sodhi and C. E. Brion, *J. Electron. Spectrosc.* **34**, 363 (1984).

¹¹C. T. Chen, *Nucl. Instrum. Methods Phys. Res., Sect. A* **256**, 595 (1987); C. T. Chen and F. Sette, *Rev. Sci. Instrum.* **60**, 1616 (1989).

¹²According to G. Hohansson, J. Hedman, A. Berndtsson, and R. Nilsson, *J. Electron. Spectrosc.* **2**, 405 (1974), the x-ray photoemission spectroscopy measured N $1s$ binding energy is 409.93 ± 0.1 eV; By comparing our N $1s \rightarrow$ Rydberg excited state of N_2 with the $2\pi \rightarrow$ Rydberg excited states of NO and extrapolating to the ionization threshold, the N $1s$ binding energy was found to be 409.938 ± 0.010 eV.

¹³The intensity for states above 408.5 eV is subjected to the uncertainty caused by the weak peaks such as N $1s \rightarrow 4p\sigma$ or the $0 \rightarrow 1$ vibrational level of N $1s \rightarrow 4s\sigma, 5p\pi, 6s\sigma, \dots$ transitions. With the aid of optical-transition data of NO, one can reduce this intensity uncertainty.

¹⁴K. P. Huber and G. Herzberg, *Molecular Spectra and Molecular Structure* (Van Nostrand, Princeton, 1979), Vol. 4, and references therein.

¹⁵N. Saito and I. H. Suzuki, *Phys. Rev. Lett.* **61**, 2740 (1988). Based on β asymmetry parameter measurements, these authors favored the assignment of peak 6 to a final state with π character. Their instrumental resolution, however, was unable to resolve peaks 6 and 7, and the π character could arise from peak 7.

¹⁶O. Edqvist, E. Lindholm, L. E. Selin, H. Sjögren, and L. Åsbrik, *Ark. Fys.* **40**, 439 (1970).